



OPEN

Tissue volume estimation and age prediction using rapid structural brain scans

Harriet Hobday¹, James H. Cole^{2,3}, Ryan A. Stanyard^{4,5}, Richard E. Daws¹, Vincent Giampietro¹, Owen O'Daly¹, Robert Leech¹ & František Váša^{1✉}

The multicontrast EPI_{mix} sequence generates six contrasts, including a T₁-weighted scan, in ~1 min. EPI_{mix} shows comparable diagnostic performance to conventional scans under qualitative clinical evaluation, and similarities in simple quantitative measures including contrast intensity. However, EPI_{mix} scans have not yet been compared to standard MRI scans using established quantitative measures. In this study, we compared conventional and EPI_{mix}-derived T₁-weighted scans of 64 healthy participants using tissue volume estimates and predicted brain-age. All scans were pre-processed using the SPM12 *DARTEL* pipeline, generating measures of grey matter, white matter and cerebrospinal fluid volume. Brain-age was predicted using *brainageR*, a Gaussian Processes Regression model previously trained on a large sample of standard T₁-weighted scans. Estimates of both global and voxel-wise tissue volume showed significantly similar results between standard and EPI_{mix}-derived T₁-weighted scans. Brain-age estimates from both sequences were significantly correlated, although EPI_{mix} T₁-weighted scans showed a systematic offset in predictions of chronological age. Supplementary analyses suggest that this is likely caused by the reduced field of view of EPI_{mix} scans, and the use of a brain-age model trained using conventional T₁-weighted scans. However, this systematic error can be corrected using additional regression of T₁-predicted brain-age onto EPI_{mix}-predicted brain-age. Finally, retest EPI_{mix} scans acquired for 10 participants demonstrated high test-retest reliability in all evaluated quantitative measurements. Quantitative analysis of EPI_{mix} scans has potential to reduce scanning time, increasing participant comfort and reducing cost, as well as to support automation of scanning, utilising active learning for faster and individually-tailored (neuro) imaging.

EPI_{mix}. A new multicontrast magnetic resonance (MR) pulse sequence has been developed, named EPI_{mix}¹. This sequence utilises single-shot echo-planar imaging (EPI) and different magnetisation preparations to rapidly generate six contrasts; T₁-FLAIR (fluid attenuated inversion recovery), T₂-FLAIR, T₂-weighted, T₂*-weighted, diffusion-weighted imaging (DWI) and apparent diffusion coefficient (ADC) (for full acquisition details, see Skare et al.¹). The EPI_{mix} sequence has lower signal-to-noise (SNR) ratio and resolution than standard MRI sequences¹, resulting in lower image quality ratings than routinely collected corresponding MR scans^{2,3}. However, the main benefit of this single-shot, multicontrast sequence over routinely acquired individual MRI sequences is its speed. The EPI_{mix} sequence is faster than corresponding single-contrast sequences because of its lower matrix size and because an EPI readout is more SNR-efficient than analogous fast spin echo (FSE) readouts¹. This multimodal sequence can acquire full brain coverage in 78 seconds, relative to the ~750 seconds needed to collect these six contrasts using standard MRI sequences^{2,3}. In addition to being more cost effective⁴, shorter scanning times improve participants' comfort and reduce motion⁵, potentially resulting in less unusable data, especially for clinical populations⁶. The EPI_{mix} sequence also generates multiple types of MR contrasts, therefore capturing more tissue characteristics than standard parametric mapping^{2,3}.

¹Department of Neuroimaging, Institute of Psychiatry, Psychology and Neuroscience, King's College London, London, UK. ²Department of Computer Science, Centre for Medical Image Computing, University College London, London, UK. ³Dementia Research Centre, Institute of Neurology, University College London, London, UK. ⁴Department of Forensic and Developmental Sciences, Institute of Psychiatry, Psychology and Neuroscience, King's College London, London, UK. ⁵Centre for the Developing Brain, School of Biomedical Engineering and Imaging Sciences, King's College London, London, UK. ✉email: frantisek.vasa@kcl.ac.uk

Quantitative analyses. To establish whether this new sequence has potential to reduce scanning time whilst producing similar derived measures, it needs to be quantitatively compared to corresponding routinely acquired MR scans. (In this context, the terms *quantitative* and *qualitative* refer to the type of analysis used, rather than the type of MR scan. Specifically, qualitative measures refer to visual inspection of scans, whereas quantitative measures refer to analyses which employ numerical computations.) Previous research established that EPI-mix scans are comparable to conventional scans in the context of qualitative clinical diagnosis^{2,3}. Moreover, our previous work compared EPI-mix and routine T₁-weighted (T₁-w) scans (Note that the EPI-mix sequence includes a T₁-FLAIR contrast, while the “conventional” single-contrast scans were acquired using an IR-FSPGR sequence. Still, as both sequences are T₁-weighted, we refer to both as such (as well as simply “T₁-w”).) using simple rapidly-derived quantitative measurements, including image intensity and Jacobian determinants (obtained from the registration to Montreal Neurological Institute (MNI) standard space), and found high similarity in these rudimentary quantitative measures as well as their potential to identify inter-individual differences⁷. (Note that the EPI-mix sequence includes a T₁-FLAIR contrast, while the “conventional” single-contrast scans were acquired using an IR-FSPGR sequence. However, both sequences are T₁-weighted and are referred to as such [as well as simply “T₁-w”).) We further demonstrated the utility of the multicontrast EPI-mix sequence to construct morphometric similarity networks (MSNs), which provide individual estimates of anatomical connectivity⁸, in minutes following participants entering the MRI scanner⁷. However, EPI-mix scans have not previously been compared to standard sequences using established quantitative structural neuroimaging measures such as estimates of tissue volume⁹ or predicted brain-age, a putative biomarker of brain health^{10,11}. Such quantitative measures likely reflect subtle inter-individual differences and provide a more thorough comparison between EPI-mix and standard sequences than qualitative measures¹² or potentially noisy estimates such as tissue intensity¹³. Moreover, the ability to derive commonly used quantitative measures from data acquired with faster imaging sequences, such as EPI-mix, has the potential to reduce scanning time, increasing participant comfort and reducing costs.

Active acquisition. One potential application of the EPI-mix sequence is in active acquisition. Active acquisition is a proposed type of data acquisition which would utilise active learning¹⁴ to analyse MRI data as it is acquired, with results used to guide further image acquisition, in a closed-circuit sequence^{15,16}. This would remove the necessity of making a priori decisions about scanning parameters such as the type of scan, scan resolution and/or the scan location. Instead, these would be dependent on the individual inside the scanner, driving the selection of scanning sequences towards identification of individual differences or personalised clinical diagnosis. In this way, active acquisition holds the potential for reduced scan time and improved accuracy, reliability and individualisation of (neuro)imaging¹⁶. The main feasibility obstacles to active acquisition are the speed of image collection as well as data processing and analysis; to realise the benefits of this multimodal adaptive approach, analyses need to be carried out in near real-time^{7,16}. Due to the relative speed of the new EPI-mix sequence, it could contribute considerably to this process.

Quantitative comparison of EPI-mix and standard T₁-w contrasts. Here, we focused on the T₁-w EPI-mix contrast and compared it to a standard T₁-w contrast at two levels. We first compared T₁-w global and voxel-wise estimates of grey matter (GM), white matter (WM) and cerebrospinal fluid (CSF) tissue volumes⁹. These tissue volumes vary as a function of age and are typically abnormal in many psychiatric and neurological populations^{17,18}.

We then compared predicted brain-ages from EPI-mix and standard T₁-w scans to assess whether EPI-mix can reliably detect the well-established relationship between healthy aging and changes in tissue volumes^{17,19}. Predicted brain-ages are derived from a validated multivariate regression model that estimates the biological age of an individual brain directly from the imaging data. This estimate provides a useful summary of the large voxel-wise spaces generated by standard high-resolution T₁-w scans into a single interpretable value. The difference between the predicted brain-age and the true chronological age is a versatile measure that has been associated with cognitive ability^{11,20} as well as clinical status and severity, with significantly “older” brain-ages associated with traumatic brain injury (TBI)²¹, mild cognitive impairment (MCI) and Alzheimer’s disease (AD)²². Furthermore, predicted brain-age could be a better predictor of disease risk than chronological age^{20,23}. For example, brain-age has been shown to be a reliable predictor of which individuals will develop AD^{24,25}.

We expected quantitative measurements derived from EPI-mix T₁-w scans, including global and voxelwise estimates of tissue volume as well as predicted brain-age, to be broadly comparable to analogous estimates derived from standard T₁-w scans. Given the notable differences in the field of view (FoV) between EPI-mix and standard T₁-w scans, the tissue volume and brain-age analyses were repeated with standard T₁-w scans that had their FoV artificially reduced to match the FoV of the EPI-mix T₁-w contrast. Finally, we assessed the within-session test-retest reliability of the EPI-mix-derived estimates of tissue volume and predicted brain-age.

Methods

Participants. EPI-mix scans (including a T₁-w contrast) were acquired for 95 healthy participants across three studies that used the same MRI scanner; one participant with particularly reduced cortical coverage (due to reduced FoV of EPI-mix scans, discussed below) was excluded, resulting in EPI-mix scans from 94 participants (F: 47, M: 47) used for analyses. The age range was 18–59 years. The mean age of participants was 28.2 years, with a standard deviation of 9.2 years (female mean age: 27.5 ± 8.6 years; male mean age 28.9 ± 9.7 years). Of those 94 participants, 64 (F: 32, M: 32) were also scanned using a standard high-resolution T₁-w sequence. The age range of this subset of participants was 18–59 years; their mean age was 28.9 years, with a standard deviation of 10.1 years (female mean age: 28.6 ± 9.6 years; male mean age: 29.3 ± 10.5 years); for details, see Supplementary

Information (SI) Fig. S1. All three studies received ethical approval from King's College London's Psychiatry, Nursing and Midwifery Research Ethics Committee (KCL Ethics References: HR-18/19-9268, HR-18/19-11058 and HR-19/20-14585). All participants gave written informed consent to take part in their respective study. All experiments were performed in accordance with relevant guidelines and regulations.

MRI acquisition. All scans were collected on the same General Electric (GE) MR750 3T scanner (Waukesha, WI). EPI-mix scans were acquired from 94 participants, consisting of six contrasts (T_2^* , T_2 -FLAIR, T_2 , T_1 -FLAIR, DWI, ADC). Only the T_1 -FLAIR contrast was used in this study (referred to as the EPI-mix T_1 -w contrast), which was acquired with the following parameters: TE = 16.5 ms, TR = 1300 ms, TI = 582 ms, flip angle = 90°, matrix size = 180 × 180, FoV 240 mm, 32 slices, slice thickness = 3 mm, voxel resolution = 0.975 × 0.975 × 3 mm, acquisition time 1 min 10 s. The EPI-mix sequence includes an in-scanner motion correction step¹ and we used the motion-corrected images for analyses. For details regarding the EPI-mix sequence, see Skare et al.¹. Additionally, for 10 participants a second EPI-mix scan was acquired during the same session, which was used to quantify test-retest reliability.

Additionally, conventional T_1 -w scans were acquired for 64 participants within the same session, using an inversion recovery-prepared fast spoiled gradient recalled-echo (IR-FSPGR) sequence. Of these, 12 scans were acquired with the following parameters: TE = 3.172 ms, TR = 8.148 s, flip angle = 12°, matrix size = 256 × 256, FoV = 256 mm, 164 slices, slice thickness = 1 mm, voxel resolution 1 × 1 × 1 mm, acquisition time 2 min 54 s; and 52 scans were acquired with the following parameters: TE = 3.016 ms, TR = 7.312 ms, flip angle = 11°, matrix size = 256 × 256, FoV = 270 mm, 196 slices, voxel resolution = 1.05 × 1.05 × 1.2 mm, acquisition time 5 min 37 s.

Pre-processing and brain-age estimation. All brain scans were pre-processed using a SPM12 DARTeL processing pipeline²⁶, including bias field correction, segmentation, registration to standard space (MNI152, 6th generation) via an intermediate study-specific template, and smoothing using a 4mm full width at half maximum (FWHM) kernel. This process generated voxelwise estimates of tissue volumes, including grey matter (GM), white matter (WM), and cerebrospinal fluid (CSF). Global tissue volumes were calculated by summing across voxels in each tissue class.

The above processing pipeline was applied as part of the *brainageR* software, which was additionally used to obtain brain age predictions using voxel-wise estimates of GM, WM and CSF tissue volume. The brain-age model was previously trained to predict chronological age from conventional T_1 -w scans in 3377 healthy people aged 18–92 years, using Gaussian Processes Regression. For additional information about the brain-age model, see Cole²⁷ and <https://github.com/james-cole/brainageR>.

The reduced FoV of the EPI-mix acquisition used in this study resulted in imperfect cortical coverage in some participants; in particular, portions of the inferior temporal and/or superior parietal lobes were not consistently scanned (SI Fig. S2). To investigate the potential impact of this reduced FoV on quantitative analyses, we repeated analyses using standard T_1 -w scans with artificially reduced FoV, to match the reduced EPI-mix FoV (within-participants). This was performed using affine registration (FSL FLIRT)²⁸ of the standard T_1 -w scan to an upsampled version of the same participant's EPI-mix T_1 -w contrast (resampled from the EPI-mix resolution of 0.975 × 0.975 × 3 mm, to match the standard T_1 -w resolution of 1 × 1 × 1 mm, or 1.05 × 1.05 × 1.2 mm). Standard T_1 -w scans with artificially reduced FoV (T_1 -w FoV_{EPI}) were then processed using the steps described above, for both tissue volume estimation and brain age prediction.

Processing was run on a Dell workstation (16-CPU 3.6GHz Intel Xeon, 128Gb RAM). Total processing time was recorded for each scan, including data processing using SPM12 and brain-age estimation. The processing time of EPI-mix T_1 -w scans was: median [1st, 3rd Quartile] (Md [Q₁, Q₃]) = 4.82 [4.75, 4.9] min; for standard T_1 -w scans, Md [Q₁, Q₃] = 7.61 [7.50, 8.17] min; for standard T_1 -w scans with reduced FoV, Md [Q₁, Q₃] = 5.42 [5.37, 5.66] min (SI Fig. S3).

Statistical analysis. Quantitative measures derived from EPI-mix T_1 -w scans, standard T_1 -w scans and T_1 -w scans with reduced FoV from 64 participants were compared using the Spearman's correlation coefficient (r_s). We first compared tissue volumes (for GM, WM and CSF) between sequences, both at the global and voxelwise levels. Voxelwise comparisons were restricted to voxels contained within the FoV of EPI-mix scans in the majority of participants (i.e. voxels with at least 0.001 mm³ tissue volume in at least 95% of participants).

Furthermore, we quantified the relationship between GM volume and participant chronological age, to ascertain whether EPI-mix T_1 -w scans are equally sensitive as standard T_1 -w acquisitions to known decreases in GM volume in ageing^{17,19}. To investigate whether associations between GM volume and age differ across contrasts, we additionally investigated differences in the strength of this association between pairs of contrasts using bootstrap. Specifically, we re-estimated Spearman's r_s and r^2 , in 10'000 samples of 64 participants, sampled with replacement from the original group. We subsequently obtained a distribution of the difference in Spearman's r_s and r^2 , between all three pairs of contrasts (i.e. EPI-mix VS T_1 -w, EPI-mix VS T_1 -w FoV_{EPI}, T_1 -w VS T_1 -w FoV_{EPI}), as well as a corresponding 95% confidence interval. Inspecting whether the confidence interval includes 0 allows us to determine whether pairs of associations differ.

We next compared estimates of predicted brain-age to true (chronological) age, across sequences, using Spearman's correlation coefficient (r_s), the proportion of variance explained (r^2) as well as the median absolute error (MAE). We also compared the predicted brain-ages between scan types.

As the correspondence between brain age predictions from standard and EPI-mix T_1 -w scans was imperfect (likely due to the brain-age model being trained on standard T_1 -w scans; see *Results & Discussion*), we explored the use of an additional regression step to optimise brain age prediction from EPI-mix T_1 -w scans. We used leave-one-out cross-validation to regress T_1 -w predicted brain-age on EPI-mix-predicted brain-age (in 63 participants),

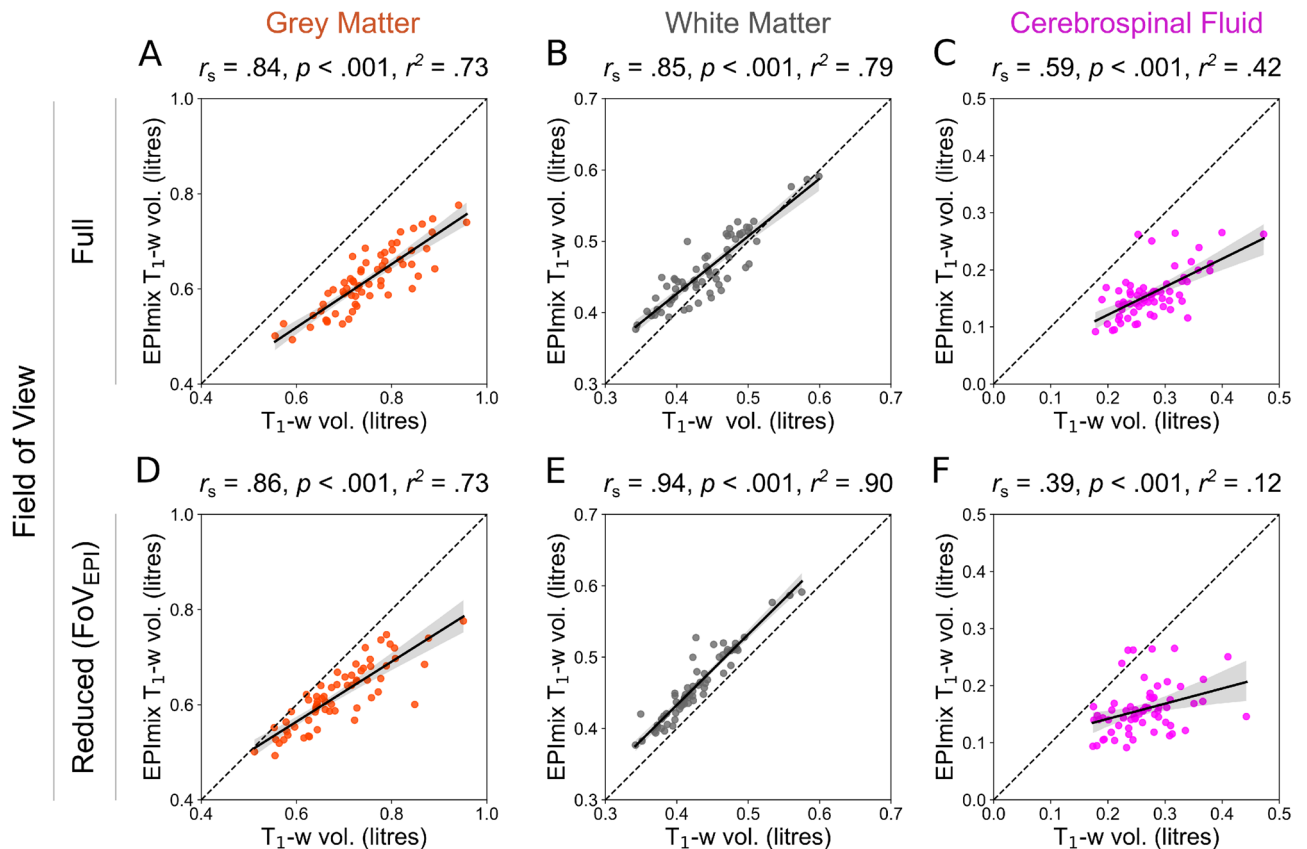


Figure 1. Global tissue volume estimation across contrasts. Comparison of tissue volumes (grey matter, white matter and cerebrospinal fluid) between T₁-w and EPI-mix (T₁-w) scans with full field of view (A–C) and between EPI-mix (T₁-w) scans and T₁-w scans with reduced field of view (D–F). (Spearman's correlation coefficient r_s , p -value, r^2 derived from Pearson's correlation).

leading to an adjusted estimate of predicted brain-age in the remaining (left-out) participant. Repeating this approach by iterating across all participants enabled us to quantify the MAE (relative to chronological age) of this adjusted brain-age estimate.

Finally, to benchmark the relative ability of each scan type (T₁-w, EPI-mix T₁-w, T₁-w FoV_{EPI}) to predict brain-age, we compared each MAE estimate to the MAE from the worst possible brain-age model. Our “null model” MAE estimate was based on an assumed prediction of the same brain-age for every participant, equivalent to the mean age of participants within the training dataset of the *brainageR* model (40.6 years); this led to a null MAE of 15.6 years. We then calculated the ratio of this null MAE to the MAE of each scan type, to estimate the extent of predictive improvement of each scan type relative to the worst possible model.

Most analyses were carried out using the sample of 64 participants for whom both EPI-mix and standard T₁-w scans were available; additionally, some analyses focused on EPI-mix T₁-w scans were repeated in the full sample of 94 participants – including the relationship between EPI-mix-derived GM volume and chronological age, and the correlation between EPI-mix-predicted age and chronological age (SI Fig. S4).

Test-retest reliability of EPI-mix T₁-w scans. Test-retest reliability of quantitative measures derived from EPI-mix T₁-w scans was assessed using 10 within-session test-retest EPI-mix scans. Test-retest reliability was evaluated using the intraclass correlation coefficient; specifically, we used the one-way random effects model for the consistency of single measurements, i.e., ICC(3,1), hereafter referred to as ICC₁²⁹. We quantified the test-retest reliability of global tissue volumes (GM, WM and CSF), corresponding voxel-wise tissue volumes, as well as predicted brain-age.

All statistical analyses were carried out in Python 3.7.

Results

Tissue volume. We first compared global brain volumes of conventional and EPI-mix-derived T₁-w scans. We observed strong positive correlations between standard T₁-w and EPI-mix T₁-w scans, in both GM volume ($r_s = 0.84$, $p < 0.001$; Fig. 1A) and WM volume ($r_s = 0.84$, $p < 0.001$; Fig. 1B). Measures of CSF volume demonstrated a weaker positive correlation ($r_s = 0.56$, $p < 0.001$; Fig. 1C). These results were qualitatively consistent when using T₁-w scans with reduced FoV (Fig. 1D–F).

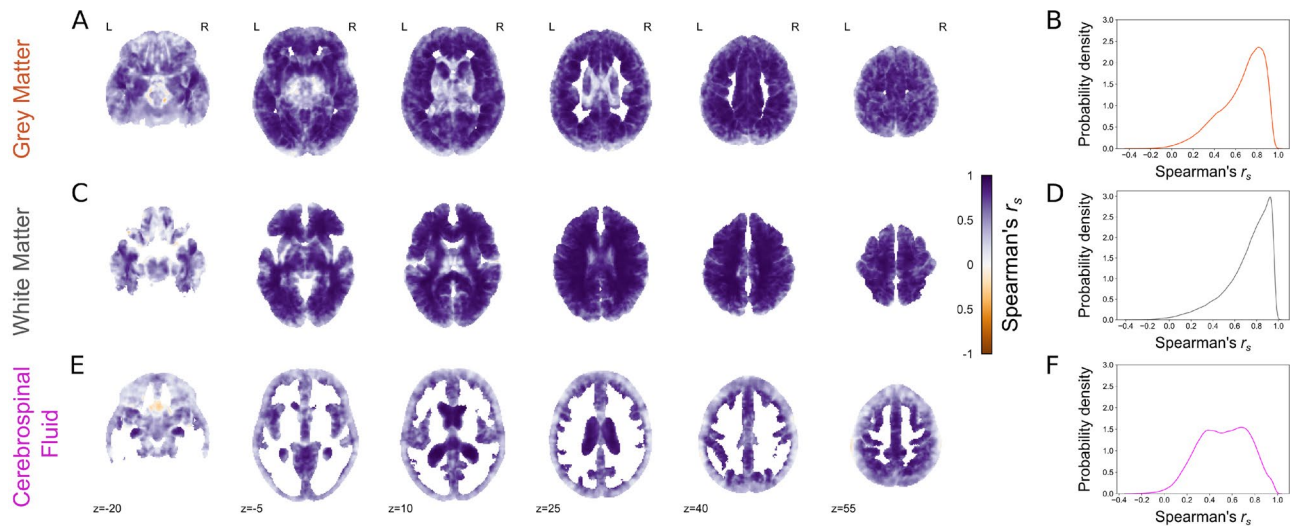


Figure 2. Voxel-wise tissue volume estimation across contrasts. Correlation between voxel-wise tissue volume estimates from T_1 -w and EPImix (T_1 -w) scans, and corresponding probability density plots, for grey matter (A, B), white matter (C, D) and CSF (E, F). Only voxels with at least 0.001 mm^3 tissue volume in at least 95% of participants are shown.

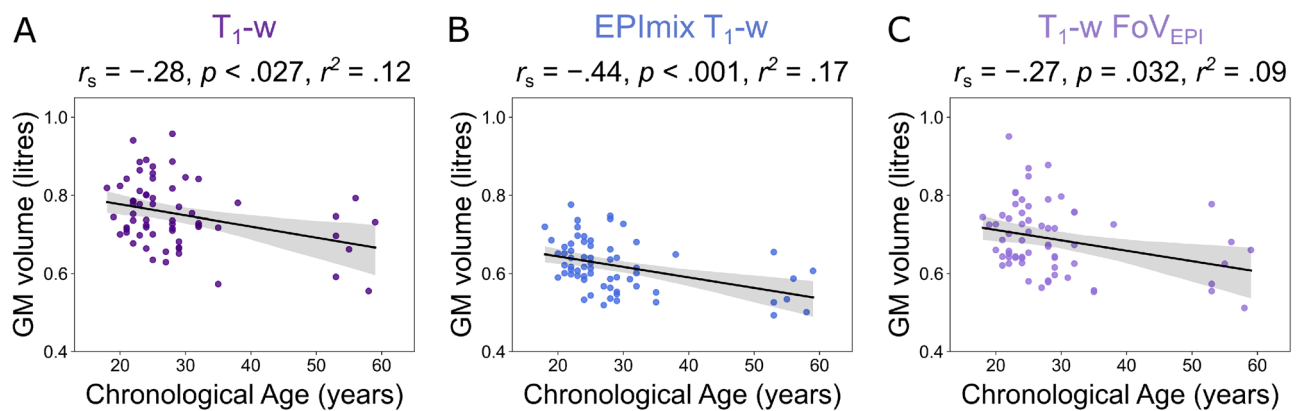


Figure 3. Grey matter volume as a function of chronological age, using volume estimates derived from (A) T_1 -w scans, (B) EPImix T_1 -w scans and (C) T_1 -w scans with reduced field of view.

We next compared voxelwise estimates of GM, WM and CSF volume between conventional and EPImix-derived T_1 -w scans, in voxels with at least 0.001 mm^3 tissue volume in at least 95% of participants. Predominantly positive correlations across participants were observed for all three tissue types. Similarly to global tissue volumes, correlations were strongest in the GM (median [1st, 3rd Quartile] (Md [Q₁, Q₃]) = 0.70 [0.52, 0.82]; Fig. 2A,B) and WM (Md [Q₁, Q₃] = 0.77 [0.62, 0.88]; Fig. 2C,D), followed by CSF (Md [Q₁, Q₃] = 0.53 [0.36, 0.70]; Fig. 2E,F).

Additionally, we quantified the relationship of global GM volume with age. GM volume decreased as a function of age, for estimates derived from standard T_1 -w scans ($r_s = -0.28$, $p = 0.027$; Fig. 3A), EPImix T_1 -w scans ($r_s = -0.44$, $p < 0.001$; Fig. 3B) and T_1 -w scans with reduced FoV ($r_s = -0.27$, $p = 0.032$; Fig. 3C). Bootstrap sampling of participants demonstrated that the association between GM volume and age for EPImix T_1 -w scans is marginally stronger than corresponding associations estimated using GM volumes derived from T_1 -w scans, and T_1 -w scans with reduced FoV. For details, see Supplementary Information.

Brain age. Following tissue volume analyses, we used a pre-trained Gaussian Processes Regression model²⁷ to quantify the relative ability of EPImix T_1 -w and standard T_1 -w scans to predict brain-age. As a first step, we compared the chronological (true) age of participants with their brain-age prediction from each type of scan. Standard T_1 -w scans showed a high correspondence between chronological and predicted age, including both a high correlation and low error ($r_s = 0.73$, $p < 0.001$, MAE = 3.72 years; Fig. 4A). EPImix T_1 -w scans also showed a high correlation between chronological and predicted age ($r_s = 0.61$, $p < 0.001$) but with a substantially higher error (MAE = 14.24 years), due to a systematic prediction offset (Fig. 4B). Additional analysis of standard T_1 -w scans with reduced FoV (to match EPImix) showed a similarly reduced correspondence between predicted and chronological age ($r_s = 0.36$, $p = 0.004$, MAE = 13.05 years; Fig. 4C), suggesting that the poorer predictive ability of EPImix T_1 -w scans was likely caused by their reduced brain coverage.

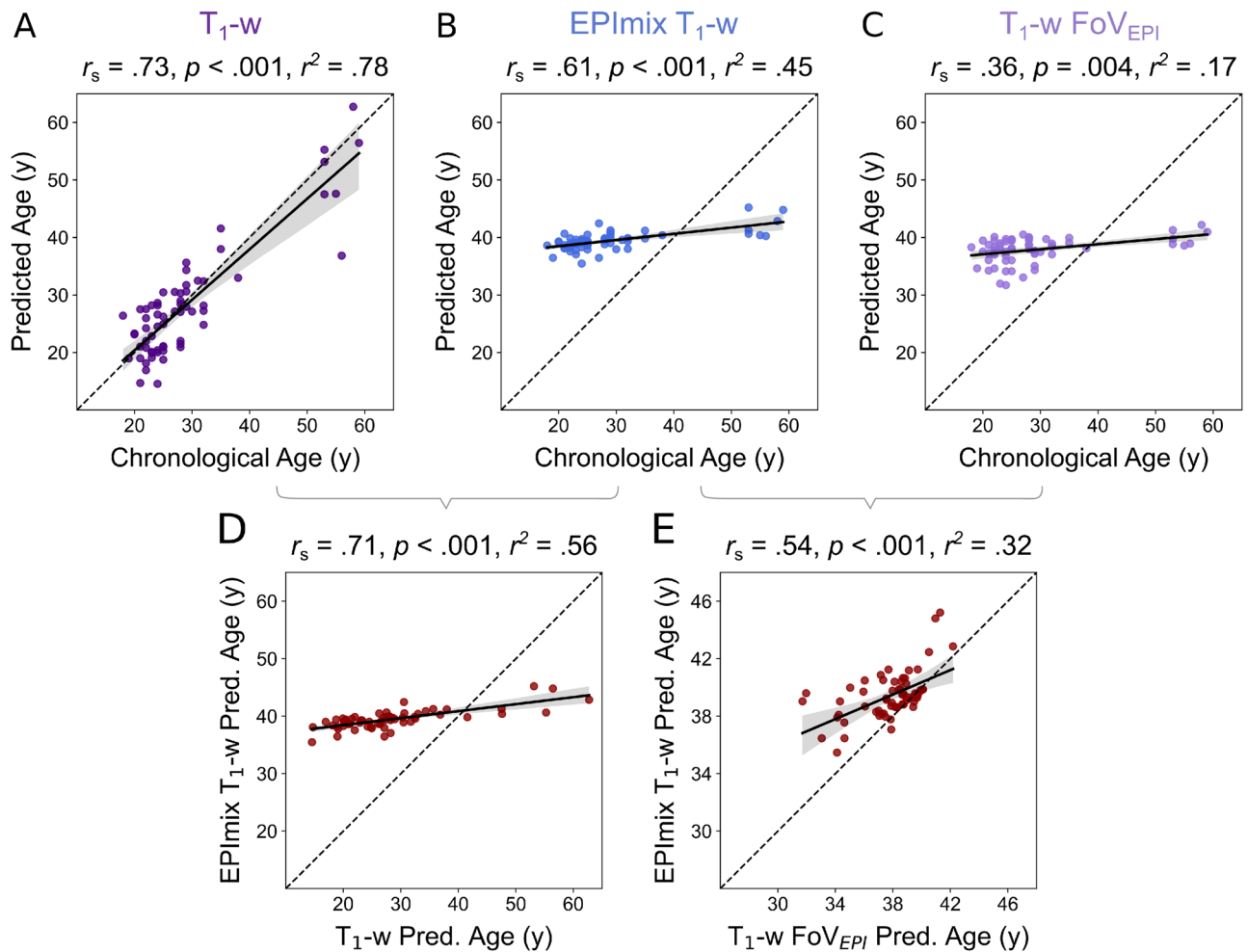


Figure 4. Age prediction across contrasts. Predicted age as a function of chronological age for (A) T_1 -w scans, (B) EPImix T_1 -w scans and (C) T_1 -w scans with reduced FoV. (D) Predicted age of EPImix T_1 -w scans compared to standard T_1 -w scans, and (E) EPImix T_1 -w scans compared to T_1 -w scans with reduced FoV. (Spearman's correlation coefficient r_s , p -value, r^2 derived from Pearson's correlation).

Furthermore, we directly evaluated the correspondence between brain-age estimates from different sequences. There was a strong positive correlation between predicted brain-age derived from EPImix T_1 -w and standard T_1 -w scans ($r_s = 0.71$, $p < 0.001$), although the same systematic offset (relative to the identity line) described above was apparent (Fig. 4D). The correlation decreased when comparing brain-age estimates from T_1 -w scans with identically reduced FoV ($r_s = 0.54$, $p < 0.001$), although data shifted closer to the identity line (Fig. 4E).

We next benchmarked the brain-age MAE of each contrast type relative to the worst possible MAE. Assuming an identical brain-age prediction for each participant, equivalent to the mean age of the *brainageR* training dataset (40.6 years), gives rise to an MAE of 15.6 years. While brain-age prediction using single-contrast T_1 -w scans is 4.20 \times better than this null benchmark, the performance of both EPImix T_1 -w scans and T_1 -w scans with reduced FoV is minimally improved (respectively 1.10 \times and 1.20 \times).

To improve brain-age prediction from EPImix T_1 -w scans, we used leave-one-out regression to adjust EPImix T_1 -w brain-age estimates. We regressed T_1 -w brain-age on EPImix brain-age (in 63 participants), leading to an adjusted estimate of predicted brain-age in the remaining (left-out) participant. Following iteration across all participants, this led to an adjusted MAE of 3.70 years (across left-out participants).

For all summary statistics related to predicted brain-age, see Table 1.

Test-retest reliability. We used a subsample of 10 participants with two (within-session) EPImix acquisitions each to quantify the test-retest reliability of all EPImix-derived quantitative measures evaluated in this study, using the intraclass correlation coefficient (ICC).

Estimates of global tissue volume showed high reliability, for GM (ICC [95% confidence interval (CI₉₅)] = 0.99 [0.99,1]), WM (ICC [CI₉₅] = 0.99 [0.98, 1]) and CSF (ICC [CI₉₅] = 0.92 [0.70,0.98]) (all $p < 0.001$).

Voxelwise estimates of tissue volume showed equally high test-retest reliability, for GM (Md [Q₁, Q₃] = 0.95 [0.90,0.97]; Fig. 5A,B), WM (Md [Q₁, Q₃] = 0.96 [0.90,0.98]; Fig. 5C,D) and CSF (Md [Q₁, Q₃] = 0.92 [0.87,0.97]; Fig. 5E,F).

Finally, brain-age estimates were equally reliable (ICC [CI₉₅] = 0.99 [0.95,1]).

	EPImix T ₁ -w	T ₁ -w	T ₁ -w FoV _{EPI}
Spearman r_s	0.61	0.73	0.36
Spearman p	< 0.001	< 0.001	0.004
r^2	0.45	0.78	0.17
MAE (y)	14.24	3.72	13.05
Null MAE ratio	1.10	4.20	1.20
LOO MAE (y)	3.70	–	–

Table 1. Correlation and Median Absolute Error between chronological age and predicted brain-age. The Null MAE ratio compares each MAE estimate to the MAE from the worst possible brain-age model (null MAE = 15.6 years, assuming identical prediction of the mean age of the *brainager* training sample for all participants). The leave-one-out (LOO) cross-validation MAE was derived using regression of T₁-w-predicted brain-age onto EPImix-predicted brain-age. For details, see *Methods* section *Statistical analysis*.

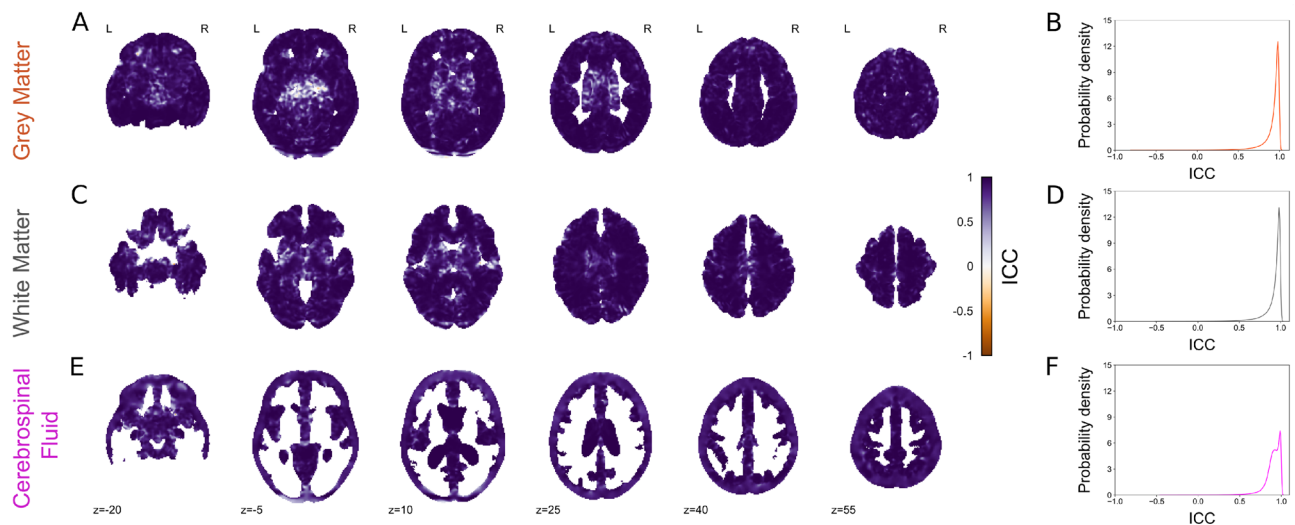


Figure 5. Test-retest reliability of EPImix (T₁-w) tissue volume estimates. Reliability of voxel-wise volume estimates, and corresponding probability density plots, in grey matter (A, B), white matter (C, D) and CSF (E, F). Test-retest reliability was evaluated using the one-way random effects model for the consistency of single measurements (ICC(3,1)²⁹). Only voxels with at least 0.001 mm³ tissue volume in at least 95% of participants are shown.

Discussion

We investigated whether T₁-w scans from the recently-developed rapid multicontrast EPImix sequence¹ are quantitatively comparable with routinely collected single-contrast T₁-w scans. For these comparisons, we relied on interpretable and widely used quantitative measures, including global and local estimates of tissue volume as well as predicted brain-age. We found a strong correspondence between tissue volumes derived from both sequences, at both the global and local levels. Moreover, estimates derived from EPImix scans showed the expected decrease in grey matter volume as a function of age. Additionally, both types of scan significantly predicted participant brain-age, although the reduced FoV of EPImix scans led to a systematic offset and a commensurate increase in prediction error. However, we demonstrated that this can potentially be corrected using additional leave-one-out regression of T₁-w-predicted brain-age onto EPImix-predicted brain-age. Finally, we used a subset of participants to show high test-retest reliability of all EPImix-derived quantitative measures evaluated in this study.

Tissue volume. Both global and voxelwise analyses showed that grey matter, white matter and cerebrospinal fluid volumes are comparable between T₁-w and EPImix T₁-w scans. This extends our previous findings of correspondence between tissue intensities and Jacobian determinants (derived from registration of T₁-w scans to MNI standard space), between EPImix and standard T₁-w scans⁷. While Jacobian determinants can be derived relatively rapidly from T₁-w scans, the primary constraint being the speed of non-linear registration, they are both less interpretable and less widely used than estimates of tissue volume. For example, recent work employing the increasingly popular approach of normative modeling^{30,31} leveraged a large sample of scans to construct normative charts of variation in brain tissue volume across the lifespan^{32,33}. Our results suggest that even volume estimates derived from rapid sequences such as EPImix could be used to anchor individual measures of brain morphology relative to such reference datasets. Our results suggest that global GM and WM volumes show higher correspondence than CSF, between EPImix and T₁-w scans, for both the full and reduced FoV (Fig. 1).

Consistently, the correspondence of CSF volumes is also reduced at the voxel level (Fig. 2E). However, some locations show high correlations between EPI mix and standard T_1 -w scans, including the ventricles, indicating value in future parsing of CSF volumes into components such as ventricular volume. Such measures are potentially more relevant to clinical translation, including demonstration of dementia progression³⁴ and differentiation of dementia variants³⁵. However, it would be preferable to increase the FoV of EPI mix scans to cover the whole brain, at the cost of a small increase in acquisition time (e.g., ~1.5 minutes instead of ~1 minute).

In addition, healthy ageing is well known to be associated with grey matter volume reduction^{17,19}. Despite our modest sample size and non-uniform distribution of participants as a function of age, we found this signature of decreasing grey matter volume in EPI mix T_1 -w scans. Bootstrap resampling of participants suggests that the association between GM volume and age in EPI mix T_1 -w scans is marginally stronger than corresponding associations estimated using standard T_1 -w scans or T_1 -w scans with reduced FoV. However, potential differences between these associations should be re-evaluated in a larger sample of participants who are uniformly distributed across age.

Tissue volumes derived from EPI mix showed high within-session test-retest reliability. Further work should investigate between-session test-retest reliability, and additionally compare test-retest reliability of EPI mix to standard high-resolution T_1 -w scans. To our knowledge, the impact of scan resolution on reliability has previously only been investigated in the context of simple statistics (e.g. mean and variance) and texture features (e.g. autocorrelation and contrast)³⁶. Further work is needed on the impact of scan resolution on reliability of more interpretable and clinically relevant quantitative measures, such as global and local tissue volumes. Translation to the clinical domain should take into account differences in reliability of tissue volume between healthy controls and clinical groups, such as individuals with MCI and AD³⁷.

Predicted brain-age. Previous research has established predicted brain-age as a putative biomarker of brain health^{10,11}. An increased predicted brain-age can be a strong predictor of risk of neurodegenerative diseases, such as Alzheimer's disease, and neuropsychiatric disorders, such as schizophrenia^{10,20,23}. We used a pre-trained Gaussian Processes Regression model²⁷ to derive estimates of predicted brain-age from EPI mix as well as conventional T_1 -w scans. EPI mix-derived brain-age showed a strong correspondence (as quantified using Spearman's r_s , and r^2) to chronological age – of a similar magnitude to previous studies (e.g. Cole²⁰) – as well as to brain-age estimated from standard T_1 -w scans.

However, a systematic offset led to a large median absolute error of the prediction. Re-analysis of T_1 -w scans with reduced FoV led to a commensurate drop in performance, confirming that this systematic error is likely caused by incomplete brain coverage of EPI mix scans, combined with the fact that the *brainageR* model we used²⁷ was pre-trained on conventional single-contrast T_1 -w scans (with full FoV). However, we showed that this systematic offset can potentially be corrected using leave-one-out regression of T_1 -w-predicted brain-age on EPI mix-predicted brain-age, to yield an adjusted estimate of EPI mix-derived brain-age. Such approaches could be used to adjust brain age predictions derived from newly-acquired EPI mix scans with reduced FoV.

In future, multicontrast data produced by the EPI mix sequence could also be used to improve the accuracy of brain age predictions and help compensate for the reduced resolution of EPI mix scans, as demonstrated by prior work on the added value of multimodal information in the context of brain age prediction²⁰. Beyond improving brain age estimates, multicontrast information provided by EPI mix could help enhance its detection of inter-individual differences.

Active acquisition. An exciting potential application for the EPI mix sequence is the active acquisition approach proposed by Cole et al.¹⁶. Active acquisition involves the online analysis of MR scans, aiming to use active learning¹⁴ to analyse scans as they are being acquired, in turn guiding subsequent acquisition steps¹⁶. As our study has found comparable quantitative measures between EPI mix and routinely collected T_1 -w scans, whilst scanning times are considerably faster, there is potential for EPI mix to be utilised in the online collection and analysis of brain scans, in the process of active acquisition.

Cole et al.¹⁶ proposed three examples of active acquisition scenarios, with EPI mix potentially being suitable for use in all three. Firstly, due to its relative speed, EPI mix could be used to rapidly acquire low resolution data to inform whether higher resolution data needs to be acquired (more slowly), depending on detection of abnormalities in the initial EPI mix scan. The other two scenarios propose to leverage multi-modal data, to classify participants and/or to identify modalities in which participants deviate the most from the norm. Due to the multicontrast nature of the EPI mix sequence, it could also be used in such scenarios. However, a larger normative sample would be required to robustly model inter-individual variability, and clinical data would be useful to test the translational relevance of such models^{30,31}.

The acquisition time of the EPI mix sequence is considerably faster than analogous single-contrast scans¹; however, the current analysis pipeline (median = 4 min 49 seconds) is too slow for real-time analysis required for active acquisition¹⁶. As it currently stands, a small amount of analyses could be carried out whilst the participant is in the scanner, to inform several additional acquisition steps. Although not sufficient for the near-real-time process of active acquisition, this could still reduce the need for participants to be recalled for follow-up scans.

In the future, there is potential to run the data analysis on more powerful computers, to speed up the processing and analysis pipeline. Alternatively, deep learning tools hold the promise of massively accelerating processing. While such models are very costly to train – in terms of time, computing power and energy – inference is very fast. Examples of relevant recent tools include *SynthSeg* for scan segmentation³⁸, *voxelmorph* for scan registration³⁹ or *FastSurfer*, a deep learning analogue of *FreeSurfer* which is particularly suitable for surface-based measures⁴⁰. Additionally, EPI mix scans could be super-resolved using image quality transfer tools, to improve scan resolution and likely increase correspondence to conventional single-contrast acquisitions⁴¹.

Methodological considerations. There are a number of methodological limitations to be considered, to maximise potential practical utility of the rapid EPImix sequence in the context of quantitative analyses.

One limitation of the present study is the reduced FoV of EPImix scans, particularly in outer areas of cortex, such as the inferior temporal lobe and superior parietal lobe. We investigated the impact of this reduced coverage on our results by re-analysing single-contrast T_1 -w scans with identically reduced FoV (on an individual participant basis). This enabled us to conclude that the reduced FoV is likely the primary hindrance in the ability of EPImix T_1 -w scans to predict brain-age. However, this issue can potentially be addressed using an additional leave-one-out regression step to correct predicted brain-age values, as demonstrated here. We relied on leave-one-out cross-validation – despite its inflated performance relative to k-fold or hold-out validation – due to small sample size, and to demonstrate the utility of even a small paired (EPImix and single-contrast T_1 -w scan) dataset for the correction of brain-age predictions in a new (EPImix-only) scan. An improved approach in future studies would be to increase the FoV of EPImix scans; despite increased scanning time, the multicontrast EPImix sequence would still remain considerably faster than routinely collected (higher-resolution) single-contrast scans. A larger FoV could be particularly important in clinical settings, where accurate diagnosis is dependent on comprehensive brain coverage⁴².

In addition, the image analysis pipeline used here remains too slow to realistically be used in an active acquisition setting, particularly if image processing needs to occur in near-real-time to drive scanning in a closed loop¹⁶. Our previous work developed a custom minimal processing pipeline which is sufficiently fast to realistically operate in near-real-time; however, this is limited to scan registration and Jacobian extraction, and does not enable quantification of tissue volume or brain age prediction. Increasing the speed of processing would be particularly valuable to enable the EPImix sequence to be used as a quantitative screening test, given that its speed is one of its main advantages over standard structural MR imaging^{1,2}. One potential avenue for the creation of custom rapid processing pipelines is Bayesian optimisation, which has previously been used to customise processing tools for brain-age prediction⁴³.

Moreover, additional research is needed to quantitatively compare the other contrasts generated by the multicontrast EPImix sequence, including T_2 -weighted, T_2 -FLAIR, T_2^* -weighted, diffusion-weighted contrasts and the apparent diffusion coefficient, with analogous single-contrast MR scans. Similarly, it would be interesting to compare EPImix to other similar sequences on scanners from other manufacturers⁴⁴, using quantitative tools applied here as well as the aforementioned deep-learning approaches.

Finally, further research should focus on clinical groups. Beyond the translational value of such studies, they would help to further investigate the correspondence between EPImix and standard T_1 -w scans. In particular, a key question is whether group differences are similar within EPImix and standard T_1 -w scans. Regarding future translation of our work to a clinical setting, it should be noted that global brain-age is a general measure, which is not disease specific. While the aim of active acquisition is to ultimately obtain a personalised diagnosis, any information regarding potential abnormality – including global deviation from expected brain-age – could help inform clinical predictions. In future, this should additionally be supplemented by more specific markers of brain health, including local estimates of brain-age^{45–48} as well as local deviations of brain anatomy from the norm^{31–33}. Accordingly, further work should compare both of these local candidate biomarkers between EPImix and standard T_1 -w scans.

Conclusion. In summary, we used popular quantitative measures derived from brain MRI to compare T_1 -w scans derived from the new rapid EPImix sequence with routinely collected single-contrast T_1 -w scans. We found that both global and voxelwise tissue volume estimates derived from EPImix T_1 -w scans were comparable with analogous measures extracted from single-contrast high-resolution T_1 -w scans. Brain age predictions from EPImix T_1 -w scans showed a strong correlation with both chronological age and brain-age estimates from single-contrast T_1 -w scans, although a systematic offset led to a high prediction error. However, this could be corrected using additional leave-one-out regression.

Taken together, our findings underline the potential of the EPImix sequence to reduce scanning time, increasing participant comfort and reducing cost, and further highlight its relevance and applicability to quantitative MR analysis routines. Future extension of this work includes the development of additional customised and deep-learning-based processing tools, as well as the analysis of other contrasts generated by EPImix; this will enable researchers to fully harness the potential of this multicontrast sequence to drive innovative paradigms in MRI acquisition and processing.

Data availability

All processing and analysis code is available on FV's GitHub, at https://github.com/frantisekvasa/epimix_volume_brain_age. Processed EPImix and single-contrast T_1 -w data, including voxel-wise tissue volumes and brain age estimates, are available at <https://doi.org/10.6084/m9.figshare.18128225>⁴⁹.

Received: 1 April 2022; Accepted: 14 June 2022

Published online: 14 July 2022

References

- Skare, S. *et al.* A 1-minute full brain MR exam using a multicontrast EPI sequence. *Magn. Reson. Med.* **3054**, 3045–3054 (2018).
- Delgado, A. F. *et al.* Diagnostic performance of a new multicontrast one-minute full brain exam (EPIMix) in neuroradiology: A prospective study. *J. Magn. Reson. Imaging*, 1–10 (2019).
- Ryu, K. H. *et al.* Clinical experience of 1-minute brain MRI using a multicontrast EPI sequence in a different scan environment. *Am. J. Neuroradiol.* **3**, 424–429 (2020).

4. Mecke, R., Wu, E. X., Meckel, S., Wetzel, S. G. & Scheffler, K. Combo acquisitions: Balancing scan time reduction and image quality. *Magn. Reson. Med.* **55**, 1093–1105. issn: 0740-3194 (2006).
5. Andre, J. B. *et al.* Toward quantifying the prevalence, severity, and cost associated with patient motion during clinical MR examinations. *J. Am. Coll. Radiol.* **12**, 689–695. issn: 1546- 1440 (2015).
6. Greene, D. J., Black, K. J. & Schlaggar, B. L. Considerations for MRI study design and implementation in pediatric and clinical populations. *Dev. Cogn. Neurosci.* **18**, 101–112. issn: 1878-9293 (2016).
7. Váša, F. *et al.* Rapid processing and quantitative evaluation of structural brain scans for adaptive multimodal imaging. *Hum. Brain Mapp.* n/a. issn: 1065-9471. <https://doi.org/10.1002/hbm.25755>. (2021).
8. Seidlitz, J. *et al.* Morphometric similarity networks detect microscale cortical organization and predict inter-individual cognitive variation. *Neuron* **97**, 231–247.e7. issn: 1097-4199 (2018).
9. Lerch, J. P. *et al.* Studying neuroanatomy using MRI. *Nat. Neurosci.* <https://doi.org/10.1038/nn.4501> (2017).
10. Cole, J. H. & Franke, K. Predicting age using neuroimaging: Innovative brain ageing biomarkers. *Trends Neurosci.* **40**, 681– 690. issn: 0166-2236 (2017).
11. Cole, J. H., Marioni, R. E., Harris, S. E. & Deary, I. J. Brain age and other bodily ‘ages’: implications for neuropsychiatry. *Mol. Psychiatry* **24**, 266–281. issn: 147–5578 (2019).
12. Pierpaoli, C. Quantitative brain MRI. *Top. Magn. Reson. Imaging*. issn: 1536-1004. https://journals.lww.com/topicsinmri/Fulltext/2010/04000/Quantitative%7B%5C_%7DBrain%7B%5C_%7DMRI.1.aspx (2010).
13. Fortin, J.-p. *et al.* Removing inter-subject technical variability in magnetic resonance imaging studies. *Neuroimage* **132**, 198– 212. issn: 1053-8119 (2016).
14. Settles, B. *Active Learning Literature Survey Computer Sciences*. Technical Report 1648 (University of Wisconsin–Madison, 2009).
15. Lorenz, R. *et al.* The automatic neuroscientist: A framework for optimizing experimental design with closed-loop real-time fMRI. *Neuroimage* **129**, 320–334. issn: 10959572 (2016).
16. Cole, J. H. *et al.* Active Acquisition for multimodal neuroimaging [version 2; peer review: 2 approved, 1 approved with reservations]. Wellcome Open Res. (2019).
17. Ramanoël, S. *et al.* Gray matter volume and cognitive performance during normal aging. *Voxel-Based Morphometry Study* <https://doi.org/10.3389/fnagi.2018.00235> (2018).
18. Wang, J. *et al.* Gray matter age prediction as a biomarker for risk of dementia. *Proc. Natl. Acad. Sci. USA.* **116**, 21213 LP –21218 (2019).
19. Hafkemeijer, A. *et al.* Associations between age and gray matter volume in anatomical brain networks in middle-aged to older adults. *Aging Cell* **13**, 1068–1074. issn: 14749726 (2014).
20. Cole, J. H. Multimodality neuroimaging brain-age in UK biobank: relationship to biomedical, lifestyle, and cognitive factors. *Neurobiol. Aging* **92**, 34–42. issn: 0197-4580 (2020).
21. Cole, J. H., Leech, R., Sharp, D. J. & Initiative, F. T. A. D. N. Prediction of brain age suggests accelerated atrophy after traumatic brain injury. *Ann. Neurol.* **77**, 571–581. issn: 0364-5134 (2015).
22. Palma, M., Tavakoli, S., Bretschneider, J. & Nichols, T. E. Quantifying uncertainty in brain-predicted age using scalaron- image quantile regression. *Neuroimage* **219**, 116938. issn: 1053-8119 (2020).
23. Franke, K. & Gaser, C. Ten years of brainAGE as a neuroimaging biomarker of brain aging: What insights have we gained? 2019. <https://doi.org/10.3389/fneur.2019.00789>.
24. Gaser, C. *et al.* BrainAGE in mild cognitive impaired patients: Predicting the conversion to Alzheimer’s disease. *PLoS One* **8**, e67346 (2013).
25. Biondo, F. *et al.* Brain-age predicts subsequent dementia in memory clinic patients. *medRxiv*, 2021.04.03.21254781 (2021).
26. Ashburner, J. *et al.* *SPM12 Manual 1–533* (Wellcome Trust Centre for Neuroimaging, 2014).
27. Cole, J. james-cole/brainageR: brainageR v2.1 version 2.1. <https://doi.org/10.5281/zenodo.3476365> (2019).
28. Jenkinson, M., Bannister, P., Brady, M. & Smith, S. Improved optimization for the robust and accurate linear registration and motion correction of brain images. *Neuroimage* **17**, 825– 841. issn: 1053-8119 (2002).
29. Chen, G. *et al.* Intraclass correlation: Improved modeling approaches and applications for neuroimaging. *Hum. Brain Mapp.* **1187–1206** (2018).
30. Marquand, A. F., Rezek, I., Buitelaar, J. & Beckmann, C. F. Understanding heterogeneity in clinical cohorts using normative models: Beyond case-control studies. *Biol. Psychiatry* **80**, 552–561. issn: 0006-3223 (2016).
31. Marquand, A. F. *et al.* Conceptualizing mental disorders as deviations from normative functioning. *Mol. Psychiatry*. issn: 1476-5578. <https://doi.org/10.1038/s41380-019-0441-1> (2019)
32. Rutherford, S. *et al.* Charting brain growth and aging at high spatial precision. *eLife* **11**, e72904. issn: 2050-084X (2022).
33. Bethlehem, R. A., Seidlitz, J., White, S. R. *et al.* Brain charts for the human lifespan. *Nature* **604**, 525–533 (2022).
34. Coupé, P., Manjón, J. V., Lanuza, E. & Catheline, G. Lifespan changes of the human brain in Alzheimer’s disease. *Sci. Rep.* **9**, 1–12 (2019).
35. Manera, A. L., Dadar, M., Collins, D. L. & Ducharme, S. Ventricular features as reliable differentiators between bvFTD and other dementias. *NeuroImage Clin.* **33**, 102947. issn: 2213- 1582 (2022).
36. Shur, J. *et al.* MRI texture feature repeatability and image acquisition factor robustness, a phantom study and in silico study. *Eur. Radiol. Exp.* **5**, 1–11 (2021).
37. Takao, H., Amemiya, S., Abe, O. & for the Alzheimer’s disease neuroimaging initiative. Reliability of changes in brain volume determined by longitudinal voxel-based morphometry. *J. Magn. Resonance Imaging* **54**, 609–616 (2021).
38. Billot, B., Robinson, E., Dalca, A. V. & Iglesias, J. E. Partial Volume Segmentation of Brain MRI Scans of any Resolution and Contrast. arXiv 2004.10221, arXiv:2004.10221 1–10 (2020).
39. Hoffmann, M., Billot, B., Iglesias, J. E., Fischl, B. & Dalca, A. V. Learning image registration without images. arXiv:2004.10282v2 (2020).
40. Henschel, L. *et al.* FastSurfer-A fast and accurate deep learning based neuroimaging pipeline. *Neuroimage* **219**, 117012. issn: 1053-8119 (2020).
41. Iglesias, J. E. *et al.* Joint super-resolution and synthesis of 1 mm isotropic MP-RAGE volumes from clinical MRI exams with scans of different orientation, resolution and contrast. *Neuroimage* **237**, 118206. issn: 1053-8119 (2021).
42. Ou, Y. *et al.* Field of View Normalization in Multi-Site Brain MRI. *Neuroinformatics* **16**, 431–444. issn: 1559-0089 (2018).
43. Lancaster, J., Lorenz, R., Leech, R. & Cole, J. H. Bayesian optimization for neuroimaging pre-processing in brain age classification and prediction. *Front. Aging Neurosci.* **10**, 28. issn: 1663-4365 (2018).
44. Polak, D. *et al.* Joint multi-contrast variational network reconstruction (jVN) with application to rapid 2D and 3D imaging. *Magn. Reson. Med.* **84**, 1456–1469 (2020).
45. Cherubini, A. *et al.* Importance of multimodal MRI in characterizing brain tissue and its potential application for individual age prediction. *IEEE J. Biomed. Health Inf.* **20**, 1232–1239 (2016).
46. Beheshti, I., Gravel, P., Potvin, O., Dieumegarde, L. & Duchesne, S. A novel patch-based procedure for estimating brain age across adulthood. *Neuroimage* **197**, 618–624 (2019).
47. Popescu, S. G., Glocker, B., Sharp, D. J. & Cole, J. H. Local brain-age: A U-net model. *Front. Aging Neurosci.* **13**. issn: 1663-4365. <https://doi.org/10.3389/fnagi.2021.761954> (2021).

48. Kaufmann, T. *et al.* Common brain disorders are associated with heritable patterns of apparent aging of the brain. *Nat. Neurosci.* **22**, 1617–1623 (2019).
49. Váša, F. Data for “Tissue volume estimation and age prediction using rapid structural brain scans”. figshare. <https://doi.org/10.6084/m9.figshare.18128225> (2022).

Acknowledgements

FV & RL would like to acknowledge support from the Data to Early Diagnosis and Precision Medicine Industrial Strategy Challenge Fund, UK Research and Innovation (UKRI). RL received support from the Wellcome/EPSCRC Centre for Medical Engineering (WT 203148/Z/16/Z). We would also like to acknowledge support from NIHR Maudsley Biomedical Research Centre (BRC) NNA08. JC acknowledges funding from a UKRI/MRC Innovation Fellowship (MR/R024790/2).

Author contributions

H.H., J.H.C., R.L. and F.V. designed the study. J.H.C., R.A.S., R.E.D., V.G., O.O'D. and R.L. collected data. H.H., J.H.C., and F.V. processed data. H.H. and F.V. performed analyses. H.H. and F.V. wrote the main manuscript text. All authors reviewed the manuscript.

Competing interests

The authors declare no competing interests.

Additional information

Supplementary Information The online version contains supplementary material available at <https://doi.org/10.1038/s41598-022-14904-5>.

Correspondence and requests for materials should be addressed to F.V.

Reprints and permissions information is available at www.nature.com/reprints.

Publisher's note Springer Nature remains neutral with regard to jurisdictional claims in published maps and institutional affiliations.



Open Access This article is licensed under a Creative Commons Attribution 4.0 International License, which permits use, sharing, adaptation, distribution and reproduction in any medium or format, as long as you give appropriate credit to the original author(s) and the source, provide a link to the Creative Commons licence, and indicate if changes were made. The images or other third party material in this article are included in the article's Creative Commons licence, unless indicated otherwise in a credit line to the material. If material is not included in the article's Creative Commons licence and your intended use is not permitted by statutory regulation or exceeds the permitted use, you will need to obtain permission directly from the copyright holder. To view a copy of this licence, visit <http://creativecommons.org/licenses/by/4.0/>.

© The Author(s) 2022